Stem Cell Reports
Article

ISSCR

OPEN ACCESS

Engineered Macroscale Cardiac Constructs Elicit Human Myocardial Tissue-like Functionality

Maria Valls-Margarit,[1,10] Olalla Iglesias-García,[2,3,10] Claudia Di Guglielmo,[2,3] Leonardo Sarlabous,[3,4,5] Karine Tadevosyan,[2,3] Roberto Paoli,[6] Jordi Comelles,[1] Dolores Blanco-Almazán,[3,4,5] Senda Jiménez-Delgado,[2,3] Oscar Castillo-Fernández,[7] Josep Samitier,[3,6,8] Raimon Jané,[3,4,5] Elena Martínez,[1,3,8,*] and Ángel Raya[2,3,9,*]

[1]Biomimetic Systems for Cell Engineering, Institute for Bioengineering of Catalonia (IBEC), The Barcelona Institute of Science and Technology, Barcelona, Spain
[2]Center of Regenerative Medicine in Barcelona (CMRB), L'Hospitalet de Llobregat, Barcelona, Spain
[3]Center for Networked Biomedical Research on Bioengineering, Biomaterials and Nanomedicine (CIBER-BBN), Barcelona, Spain
[4]Biomedical Signal Processing and Interpretation, Institute for Bioengineering of Catalonia (IBEC), The Barcelona Institute of Science and Technology, Barcelona, Spain
[5]Department of Automatic Control, Universitat Politècnica de Catalunya - BarcelonaTech (UPC), Barcelona, Spain
[6]Nanobioengineering, Institute for Bioengineering of Catalonia (IBEC), The Barcelona Institute of Science and Technology, Barcelona, Spain
[7]Institute of Microelectronics of Barcelona, IMB-CNM (CSIC), Campus UAB, Bellaterra, Spain
[8]Department of Electronics and Biomedical Engineering, University of Barcelona (UB), Barcelona, Spain
[9]Institució Catalana de Recerca i Estudis Avançats (ICREA), Barcelona, Spain
[10]Co-first author
*Correspondence: emartinez@ibecbarcelona.eu (E.M.), araya@cmrb.eu (Á.R.)
https://doi.org/10.1016/j.stemcr.2019.05.024

SUMMARY

In vitro surrogate models of human cardiac tissue hold great promise in disease modeling, cardiotoxicity testing, and future applications in regenerative medicine. However, the generation of engineered human cardiac constructs with tissue-like functionality is currently thwarted by difficulties in achieving efficient maturation at the cellular and/or tissular level. Here, we report on the design and implementation of a platform for the production of engineered cardiac macrotissues from human pluripotent stem cells (PSCs), which we term "CardioSlice." PSC-derived cardiomyocytes, together with human fibroblasts, are seeded into large 3D porous scaffolds and cultured using a parallelized perfusion bioreactor with custom-made culture chambers. Continuous electrical stimulation for 2 weeks promotes cardiomyocyte alignment and synchronization, and the emergence of cardiac tissue-like properties. These include electrocardiogram-like signals that can be readily measured on the surface of CardioSlice constructs, and a response to proarrhythmic drugs that is predictive of their effect in human patients.

INTRODUCTION

Cardiac tissue engineering aims at producing constructs with structural, physiological, and functional properties resembling human native cardiac tissue. Ultimately, such *in vitro* models will find applications in disease modeling, drug screening, and toxicology, and replacing or regenerating damaged heart tissue. The structural organization of the cardiac tissue is complex, comprising a vast array of diverse cell types (including fibroblasts, cardiac myocytes, and smooth muscle, pacemaker, and endothelial cells), arranged in a precise and stereotypical architecture to ensure that the critical function of pumping blood throughout the body is maintained (Chien et al., 2008). Efficient blood pumping requires the ~5 billion cardiomyocytes that make up an average human adult heart contracting and relaxing in a coordinated and timely order. Multiscale structural features characteristic of the heart's intracellular and intercellular organization enable the necessary coordination for the entire heart muscle to form a functional syncytium (Hunter et al., 2003). This results in electrochemical processes of such magnitude that generate voltage potentials of ~1 mV, easily recorded on the body surface. That the shape of these voltage potential waves (electrocardiogram [ECG]) is a reliable indicator of cardiac performance, used on a routine basis in clinical cardiology for over a century (Fermini and Fossa, 2003), clearly attests to the intimate dependence of structure and function in the heart.

Due to the high dependence found between cardiac muscle structural organization and its function, it has been hypothesized that growing cardiac constructs in engineering systems mimicking relevant physicochemical stimuli found *in vivo* would be advantageous to achieve tissue-like properties (Fleischer et al., 2017). In the last years, tissue-engineering methods have significantly advanced in generating functional 3D cardiac constructs (Radisic et al., 2004a; Shimizu et al., 2002; Zimmermann et al., 2002). A key issue that has deserved much attention in this field is the degree of cardiomyocyte maturation achieved within the engineered cardiac constructs (reviewed in Parsa et al., 2016). This issue is particularly important when using cardiomyocytes derived from pluripotent stem cells (PSCs), which are typically immature, fetal-like under standard two-dimensional (2D)

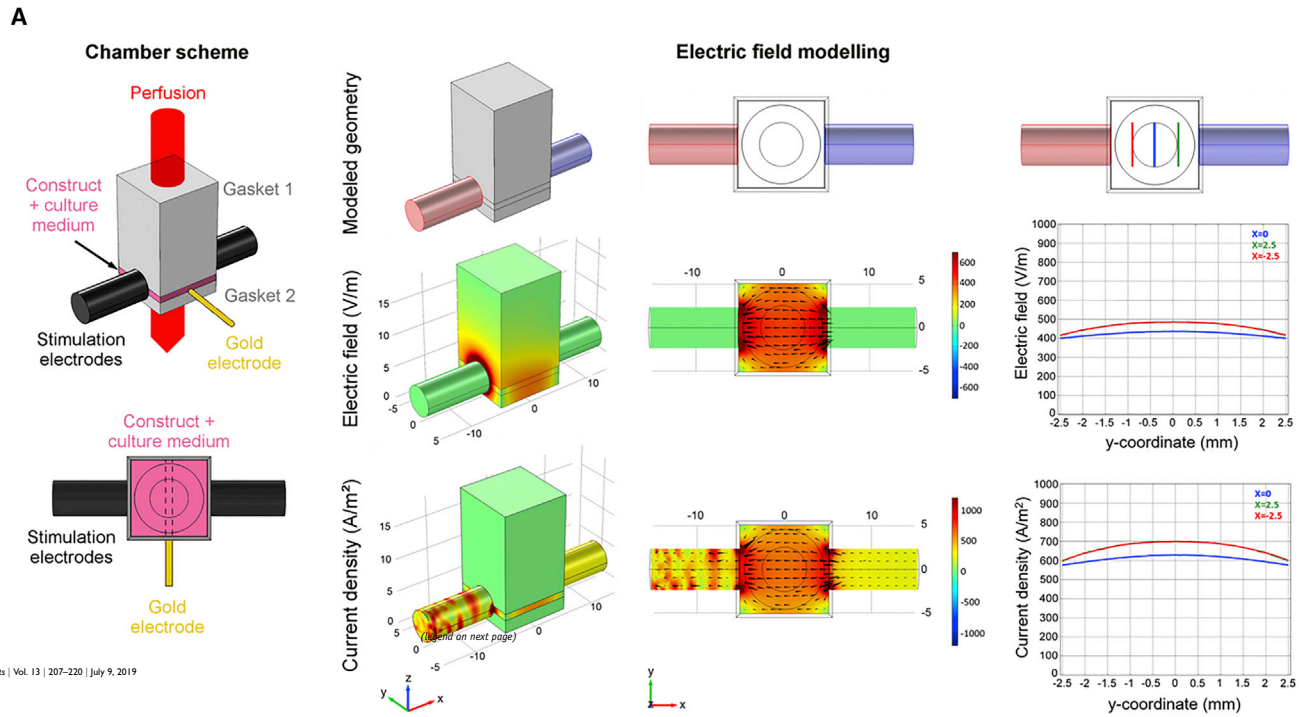
A
Chamber scheme
Perfusion
Construct + culture medium
Gasket 1
Gasket 2
Stimulation electrodes
Gold electrode
Construct + culture medium
Stimulation electrodes
Gold electrode
Modeled geometry
Electric field (V/m)
Current density (A/m²)
(legend on next page)
Electric field modelling
Electric field (V/m)
y-coordinate (mm)
X=0
X=2.5
X=-2.5
Current density (A/m²)
y-coordinate (mm)
X=0
X=2.5
X=-2.5

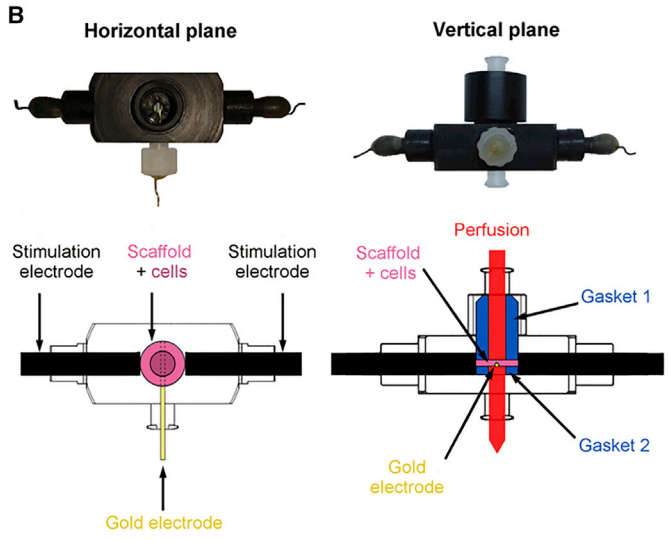
B
Horizontal plane
Vertical plane
Stimulation electrode
Scaffold + cells
Stimulation electrode
Gold electrode
Perfusion
Scaffold + cells
Gasket 1
Gasket 2
Gold electrode

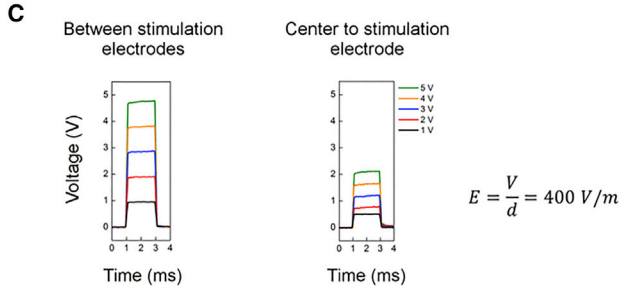
C
Between stimulation electrodes
Center to stimulation electrode
Voltage (V)
Time (ms)
Time (ms)
5 V
4 V
3 V
2 V
1 V
$E = \frac{V}{d} = 400\ V/m$

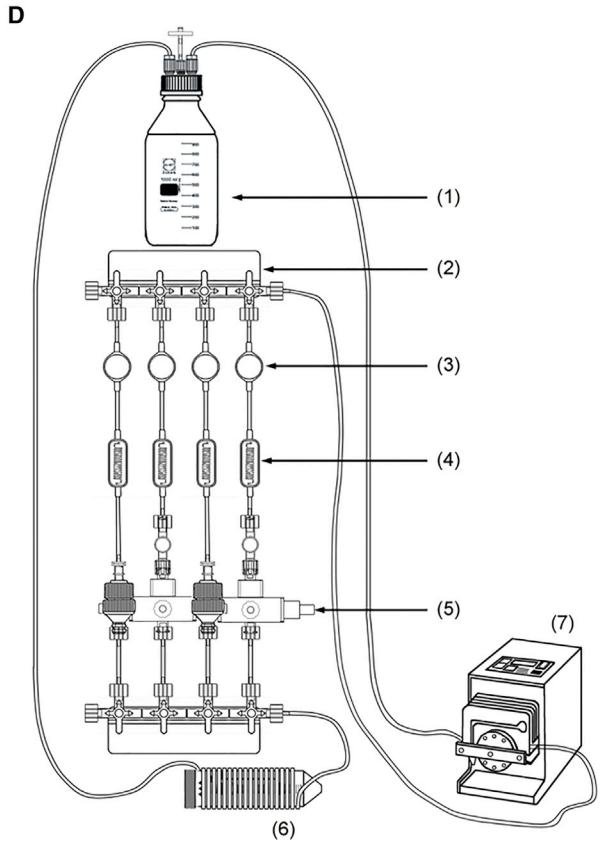
D
(1)
(2)
(3)
(4)
(5)
(6)
(7)

differentiation conditions (Feric and Radisic, 2016). Human engineered cardiac constructs developed thus far recapitulate some of the structural complexity and electromechanical functionality of the native myocardium, leading to improved performance compared with standard 2D *in vitro* cultures (Ma et al., 2015; Nunes et al., 2013; Schaaf et al., 2011; Thavandiran et al., 2013). Exogenous stimuli such as mechanical and electrical signals have been shown to further improve the electrophysiological properties, the cellular and ultrastructural organization, and the expression of cardiac-specific proteins of cardiac constructs (Godier-Furnemont et al., 2015; Radisic et al., 2004a; Tandon et al., 2009). These strategies have resulted in microengineered models of human cardiac muscle, which emerged as promising platforms for preclinical toxicology and drug screening assays (Amano et al., 2016; Hansen et al., 2010; Mathur et al., 2015). However, microtissues are minimal units with some cardiac functionality, but are inherently limited in size and cannot fully capture the complexity of the native cardiac tissue structure (Kurokawa and George, 2016). Unfortunately, the production of human macroscale tissues displaying *in vivo*-like complexity and, therefore, tissue-like functionality, is still an unmet challenge (Fleischer et al., 2017).

The design of tissue-engineering constructs on the macroscale (greater than 300 μm in thickness) is met with the challenge that effective mass transfer cannot rely on passive diffusion alone (Lovett et al., 2009). This is critical for cardiac tissue constructs due to the comparatively high metabolic demand of cardiac muscle cells, which requires a controlled microenvironment with the appropriate supply of oxygen and nutrients (Carrier et al., 2002; Radisic et al., 2004b, 2008). Perfusion bioreactor systems pioneered in Vunjak-Novakovic's laboratory have proved to be valuable in the generation of thick cardiac tissue constructs full of viable cells with aerobic metabolism (Radisic et al., 2004b). Here, we have designed and implemented a platform to produce macrotissues of engineered cardiac muscle from human PSCs, which we termed "CardioSlice." PSC-derived cardiomyocytes differentiated under standard 2D conditions were seeded, together with human fibroblasts, into 3D porous scaffolds of 10 mm in diameter and 1 mm in thickness. Constructs were cultured for up to 14 days in a parallelized perfusion bioreactor equipped with custom-made culture chambers endowed with electrostimulation capabilities. The constructs obtained developed into macroscopically contractile structures in which cardiomyocytes showed signs of increased cell maturation compared with those cultured under 2D conditions, and similar to those of microtissues. More importantly, continuous electrical stimulation of the cardiac macrotissues for 2 weeks promoted cardiomyocyte alignment and synchronization, and the emergence of cardiac tissue-like properties. These translated into spontaneous electrical activity that could be readily measured on the surface of CardioSlice constructs as ECG-like signals, and a response to proarrhythmic drugs that was predictive of their effect in human patients.

RESULTS

Development of a Parallelized Bioreactor for Continuous Perfusion and Electrical Stimulation/Recording of Cardiac Macroscale Constructs

To generate CardioSlice constructs, we designed a parallelized perfusion bioreactor including electrical stimulation (Figure 1). Our a priori design requirements included: (1) suitability for the perfusion of macroscale constructs (10 mm in diameter and 1–2 mm in thickness); (2) capability for *in vivo*-like electrical stimulation; (3) ability to produce interstitial flow with proper shear; (4) amenability to parallelization for the simultaneous culture of multiple constructs; and (5) on-line recording of the construct

Figure 1. Parallelized Perfusion Bioreactor for the Generation of CardioSlice Constructs

(A) Scheme of the custom-made perfusion chamber and 3D modeling of the electric field generated when applying a differential voltage of 5 V. The chamber scheme depicts two stimulation electrodes (black), one at each side of the construct (pink), and a central gold electrode (yellow) underneath the construct acting as internal reference. Two gaskets (gray) hold the construct in place and direct the fluid (red) flow through the scaffold. This scheme of the chamber is used to model the electrical field. Electrode configuration (red and blue cylinders in the geometry, positive and negative, respectively) and predicted electric field and current density values are displayed both in 3D and top views. Black arrowheads indicate the direction of the electric field. Plots show electric field and current density values at the positions where cells are seeded in the scaffold (central circle in the top view) (from $x = -2.5$ to $x = 2.5$).

(B) Horizontal and vertical planes of the perfusion chamber with electrical stimulation. The cardiac construct (scaffold + cells; pink) is held in place by two gaskets (blue). Black rectangles represent graphite electrodes, and the yellow rectangle and dot represent the gold electrode. Interstitial flow of culture medium (red arrow) is routed through the pores of the construct.

(C) Voltage measurements in the perfusion chamber with electrical stimulation. Measured electric field values match the values predicted by the model.

(D) Overall view of the parallel bioreactor system: medium reservoir (1), luer manifold (2), de-bubblers (3), flow restrictors (4), perfusion chambers (5), gas exchanger (6), and peristaltic pump (7). The bioreactor supports the culture of up to four cardiac constructs simultaneously.

electrical activity. To address these requirements, we first formulated an electric field model to determine the appropriate size and allocation of the stimulating electrodes within the chamber (Figure 1A). We simulated the electric field and current density generated by two graphite electrodes (5 mm in diameter) separated 1 cm apart and in contact with culture medium. Solving the model resulted in an electric field of around 400 V/m and a current density of around 600 A/m^2 in the center of the chamber, when a differential voltage of 5 V was applied. Similar values were obtained for the entire region intended for use to allocate the cardiac construct containing cells, thus making this configuration suitable for cardiomyocyte stimulation in terms of magnitude and uniformity according to the literature (Barash et al., 2010; Tandon et al., 2009). We then fabricated custom-made perfusion chambers including electrodes with the specifications included in the simulation (Figure 1B). Upon fabrication, we measured the voltage values in the actual perfusion chamber to verify that the expected stimuli were properly delivered (Figure 1C). Rectangular pulses at 3 Hz of frequency, 2 ms of duration, and increasing differential voltages from 1 to 5 V were applied to the chamber. Electric potentials between stimulating graphite electrodes and between each electrode and the center of the chamber (gold electrode) were measured. The intended waveform was reliably applied for all voltages tested. Moreover, when applying 5 V between graphite electrodes, 2 V were measured in the center of the chamber, representing an electric field of 400 V/m, in agreement with the values predicted by the model.

The shear stress to which cells would be exposed in the perfusion bioreactor was calculated as previously described (Radisic et al., 2008). The minimum flow rate needed for efficiently perfusing cardiac macrotissues depends on the overall mass balance of oxygen, and was estimated to be 0.1 mL/min for rat cardiac tissue constructs and 0.2 mL/min for human cardiac tissues. Shear stress affecting the cells within the scaffold was then calculated by taking into account the flow rate, culture medium viscosity (0.0078 dyn•s/cm^2) (Bacabac et al., 2005), and the volume (19.6 mm^3), void fraction (0.94), and mean pore radius (8.5 μm, Figure S1A) of the scaffold. Perfusion of culture medium at 0.1 mL/min evoked a shear stress of around 0.7 dyn/cm^2 while perfusion at 0.2 mL/min yielded a shear stress of around 1.3 dyn/cm^2. According to the literature, the values selected for the perfusion flow rate are sufficient to satisfy mass transport requirements associated with cardiac muscle tissue (Radisic et al., 2008), while the associated shear stress values do not compromise cardiomyocyte functionality and viability (Cheng et al., 2009; Radisic et al., 2008; Shachar et al., 2012).

Next, the custom-made perfusion chambers including electrical stimulation were installed in the parallelized perfusion bioreactor (Figure 1D). Parallelization of the culture system allowed the production of multiple cardiac macrotissues under the same physicochemical conditions and from the same pool of cells. Fluidic restrictors were installed ($R_{restrictor} \sim 10^{13} >> R_{manifold} \sim 10^7$) to ensure that the flow was homogeneously distributed through all branches. Finally, on-line recording of the electrophysiological activity of cardiac tissue constructs was carried out using the two graphite electrodes used for electrical stimulation (one acting as the source and the other one as the reference), and a gold electrode as an internal reference (Figures 1B and S1B). Recorded signals were amplified and noise-filtered to obtain the electrical activity of the constructs.

Structural Signs of Cell and Tissue Maturation in CardioSlice Constructs

To create human cardiac macrotissues, we differentiated cardiomyocytes from human induced PSCs (hiPSCs) following a robust and reproducible protocol based on modulation of Wnt/β-catenin signaling with small-molecule inhibitors (Lian et al., 2013). hiPSCs differentiated in this way formed contracting monolayers comprising high percentages of cardiomyocytes, as defined by coexpression of cardiac troponin I (cTnI) and myosin heavy chain (MHC) proteins (71.6% ± 5.3% cTnI$^+$/MHC$^+$ cells) after 20 days of differentiation (Figure S2). In preliminary studies, we determined that fully differentiated cardiomyocytes (i.e., after 20 days of differentiation from hiPSCs), but not undifferentiated hiPSCs or early committed mesoderm progenitors (as defined by the expression of T/Brachyury), could be cultured within the porous scaffolds under continuous perfusion for up to 21 days while maintaining a differentiated phenotype (data not shown). We also verified that addition of fibroblasts to iPSC-derived cardiomyocytes improved the reproducibility of obtaining viable cardiac constructs, in agreement with previous studies (Amano et al., 2016; Liau et al., 2017; Tiburcy et al., 2017). Based on those preliminary results, for the present studies we used a mixture of hiPSC-derived cardiomyocytes and human dermal primary fibroblasts seeded in a 7:1 ratio. We chose a commercial, clinical-grade porous scaffold made up of collagen and elastin to culture the cells, on account of its biocompatibility and myocardium-like pore size and stiffness (Figure S1A). A total of 5 million cells were seeded into the scaffolds using an on-purpose designed perfusion loop (see details in Experimental Procedures and Figure S1B).

In a first set of experiments, we tested the effects of electrical stimulation on human cardiac macrotissues. For this purpose, constructs were introduced into perfusion chambers and randomly assigned to the control group

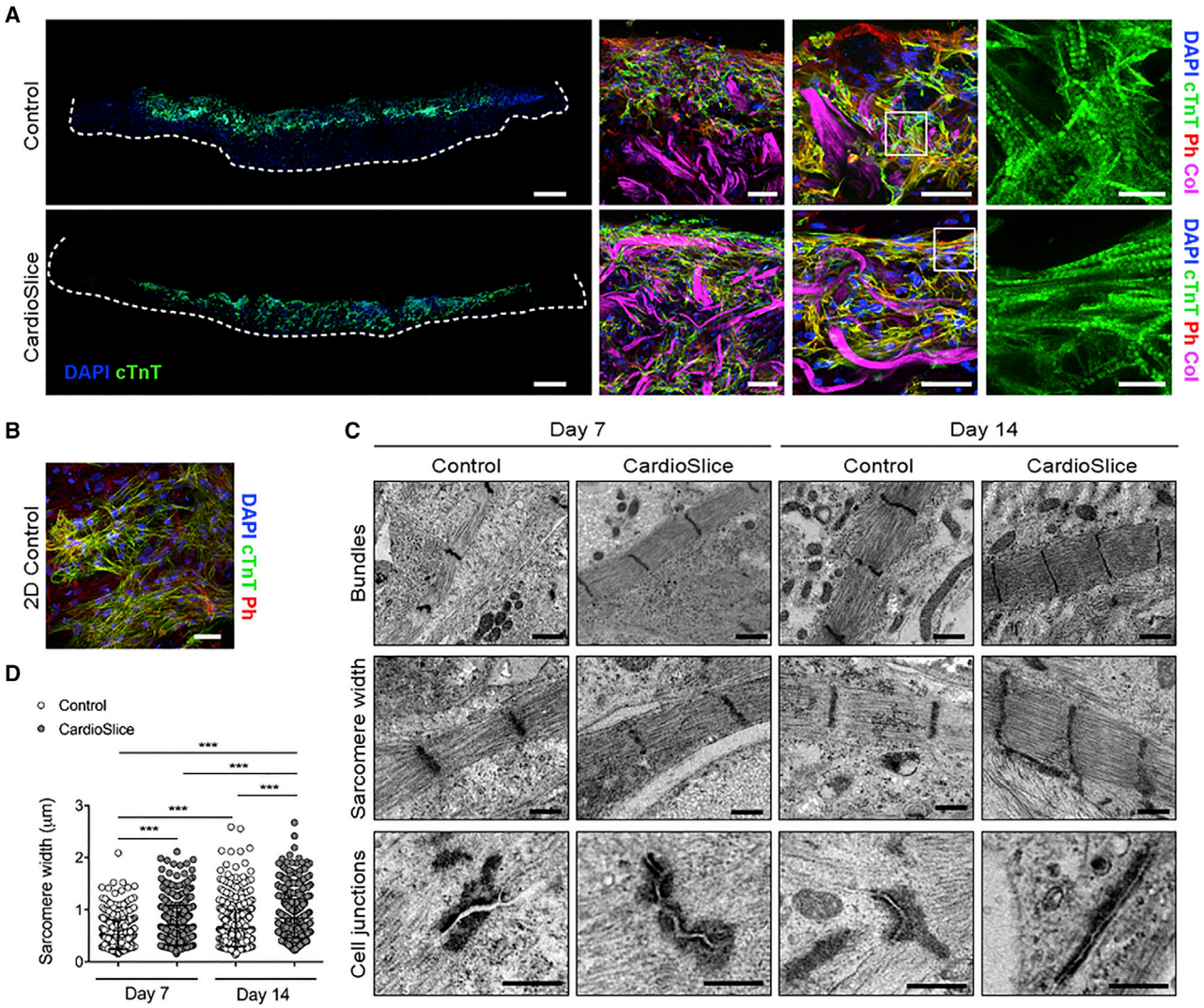

Figure 2. Morphology and Ultrastructural Organization of Human Cardiac Macrotissues

(A) Representative cross-sections of cardiac constructs after 14 days of culture without (Control) or with electrical stimulation (CardioSlice). hiPSC-derived cardiomyocytes positive for cardiac troponin (cTnT; green) and phalloidin (Ph; red) were detected in the scaffold. Nuclei were stained with 4′,6-diamidino-2-phenylindole (DAPI; blue). Cardiac macrotissues were analyzed by Second Harmonic Generation for the detection of collagen (Col; violet). Scale bars, 500 μm (left); higher magnifications (left to right), 100 μm, 50 μm, and 10 μm, respectively.

(B) Standard 2D culture of hiPSC-derived cardiomyocytes in monolayer. Cardiomyocytes were positive for cardiac troponin (cTnT; green) and phalloidin (Ph; red). Scale bar, 50 μm.

(C) Ultrastructural analysis of hiPSC-derived cardiac macrotissues. Representative transmission electron microscopy images of cardiac macrotissues after 7 and 14 days of culture. Scale bars, 1 μm (bundles) and 0.5 μm (sarcomere width and cell junctions).

(D) Morphometric analysis showing sarcomere width. Each individual sarcomere width is represented as a dot in the graph and at least 200 sarcomeres per independent experiment were measured in three independent experiments (***$p < 0.001$, $N = 3$, $n \geq 200$ per group; Mann-Whitney U test). Data are expressed as mean ± standard deviation (SD).

(only perfusion) or the CardioSlice group (perfusion and electrical stimulation), and maintained in culture for up to 14 days. Human cardiac macrotissues exhibited cardiomyocytes and fibroblasts distributed throughout the scaffold thickness (Figure S3A). Cardiomyocytes strongly expressed cardiac contractile proteins, including cardiac troponin T (cTnT) and α-sarcomeric actin (Figure 2A), with signs of increased cardiomyocyte maturation compared with cells cultured for the same time period under conventional 2D conditions (Figure 2B). No differences

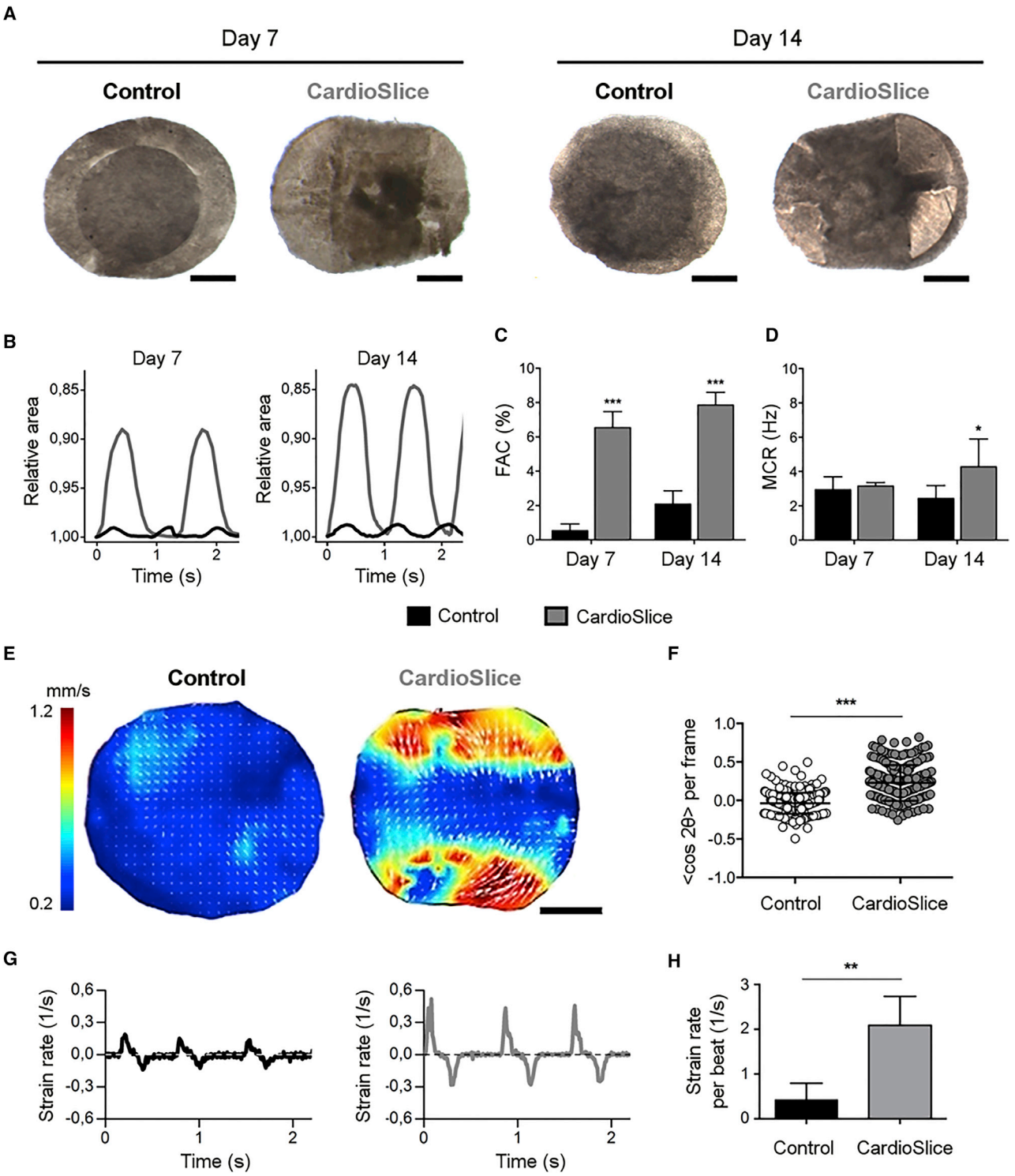

Figure 3. Functional Assessment of Human Cardiac Macrotissues

(A) Top-view images of human cardiac macrotissues after 7 and 14 days of culture, both without (Control) or with (CardioSlice) electrical stimulation. Scale bars, 2.5 mm.

(B) Contraction amplitude analysis of Control and CardioSlice constructs after 7 and 14 days of culture. Area oscillation is represented over time.

(legend continued on next page)

in cardiomyocyte proliferation or viability, as judged by the number of Ki67-positive cardiomyocytes and the number of TUNEL-positive cardiomyocytes, respectively, were found when comparing CardioSlice and control constructs after 14 days of culture (Figures S3B and S3C). Cardiomyocytes in CardioSlice constructs were mostly aligned along the direction of electric field vector used for stimulation, in contrast with the random distribution found in control constructs (Figure 2A), a finding also observed in rat-derived cardiac macrotissues (Figure S4A). At the ultrastructural level, cardiomyocytes in CardioSlice constructs displayed a statistically significant increase in sarcomere width compared with those in control constructs, after both 7 and 14 days in culture (day 7: 0.70 ± 0.38 μm for CardioSlice and 0.52 ± 0.29 μm for control; day 14: 0.83 ± 0.38 μm for CardioSlice and 0.64 ± 0.35 μm for control; $p < 0.001$) (Figures 2C and 2D), indicating a higher degree of maturation. Moreover, after 14 days in culture, more developed intercalated discs were detected in CardioSlice than in control constructs (Figure 2C). This was again in agreement with the improved ultrastructural signs of cardiomyocyte maturation observed in rat-derived cardiac macrotissues, where wider sarcomeres and better developed intercalated discs were present in electrostimulated compared with control constructs (Figures S4B and S4C).

The expression level of key cardiac genes was measured in control and CardioSlice constructs and compared with those of cells cultured for equivalent periods of time under conventional 2D conditions (Figure S3D). As expected, maturity-related cardiac genes (*MYH7*, *ACTC1*, *TNNT2*, *MLC2V*, *GATA4*, and *GJA1*) and genes encoding cardiac ion channels (*RYR2*, *SERCA2A*, *CACNA1C*, *SCNA5A*, *KCNH2*, and *KCNQ1*) were expressed under all conditions analyzed. However, no conspicuous differences were noted in cells cultured under either 2D or 3D conditions when comparing control and CardioSlice constructs (Figure S3D). Overall, the expression levels of maturity-related cardiac genes and cardiac ion channels were more similar to those of fetal human heart than to those of adult ventricular tissue, consistent with previous analyses of human iPSC-derived cardiomyocytes (reviewed in Yang et al., 2014). These results indicate that any differences observed in the functionality of cardiac macrotissues should be attributed to changes in the maturation of the multicellular structure rather than to the maturation of its individual cellular constituents.

Biomechanical Signs of Tissue Maturation in CardioSlice Constructs

Upon harvesting, both control and CardioSlice constructs displayed spontaneous beating, which was much more apparent macroscopically in the case of CardioSlice constructs (Videos S1, S2, S3, and S4). We did not find differences in the spontaneous beating rate between CardioSlice and control constructs, which we monitored after 4, 7, and 14 days of culture, and ranged from 0.6 to 1.1 beats/s. Electric field stimulation had a direct impact on cell distribution within the CardioSlice constructs, as cells concentrated in the region were delimited by the stimulating electrodes (Figure 3A). The amplitude of contraction, determined by measuring the changes in the fractional area during spontaneous beating, was significantly higher in CardioSlice constructs compared with control ones (day 7: 6.54% ± 0.94% for CardioSlice constructs compared with 0.54% ± 0.09% for control constructs; day 14: 7.85% ± 0.75% for CardioSlice constructs compared with 2.08% ± 0.12% for control constructs; $p < 0.001$), indicating improved maturation of the electromechanical coupling machinery (Figures 3B and 3C). Consistently, CardioSlice constructs also exhibited significantly higher values for the maximum capture rate (MCR) parameter when compared with control samples. This was evident after 14 days of culture: 4.28 ± 1.63 Hz in CardioSlice constructs versus 2.43 ± 0.75 Hz in control constructs ($p < 0.001$) (Figure 3D). The effects of continuous electric stimulation were not specific to human cells, since similar

(C) Bar chart showing the percentage of fractional area change (FAC) for each cardiac macrotissue (average ± SEM) (***$p < 0.001$, $N \geq 3$, $n \geq 3$ per group; Mann-Whitney U test).

(D) Maximum capture rate (MCR) of Control and CardioSlice constructs after 7 and 14 days of culture (average ± SD) (***$p < 0.001$, $N \geq 3$, $n \geq 3$ per group; Mann-Whitney U test).

(E) Representative velocity maps of beating human cardiac macrotissues after 14 days of culture. Red colors and longer arrows represent higher velocities, while blue colors and shorter arrows represent lower velocities. Scale bar, 2.5 mm.

(F) Analysis of the alignment between beating direction of human cardiac macrotissues and direction of the electric field. The order parameter $\langle \cos 2\theta \rangle$ was used, with values close to 0 meaning random distribution and values close to 1 meaning parallel alignment (average ± SD) (***$p < 0.001$, $N = 4$, $n \geq 4$ per group; Mann-Whitney U test).

(G) Strain rate of representative macrotissues over time. The curve is obtained by integrating the local strain rate (e.g., local area change per frame) over the whole construct at every time point. Positive and negative values correspond to contractions and relaxations, respectively.

(H) Strain rate per beat (average ± SD) (**$p < 0.01$, $N = 4$, $n \geq 4$ per group; one-way ANOVA). The positive values of the strain rate (contractions) were integrated over time and divided by the number of beats.

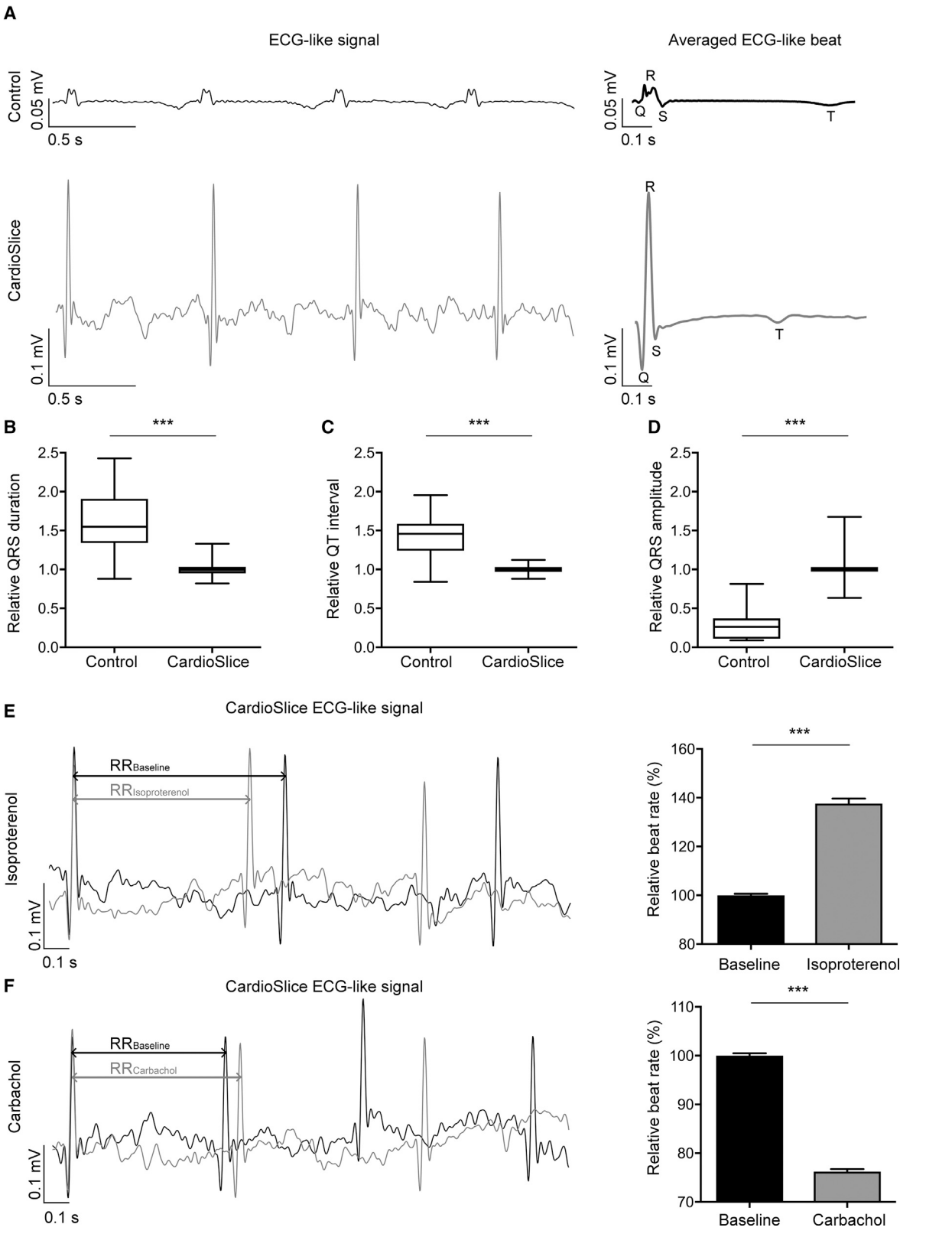

(legend on next page)

improvements in contractile behavior were obtained with rat-derived cardiac constructs (Figures S4D–S4F).

Velocity maps generated with particle image velocimetry demonstrated that the velocity in each contraction was higher in CardioSlice constructs than in controls, corroborating their enhanced contractile performance (Figure 3E). Directionality of contractions was calculated by determining the alignment of velocity vectors with respect to the direction of the stimulating electric field, and expressed by the order parameter $\langle \cos 2\theta \rangle$ (Figure 3F). CardioSlice constructs contracted parallel to the direction of the electric field applied during culture ($\langle \cos 2\theta \rangle$ close to 1), whereas control constructs displayed random distribution of velocity vectors ($\langle \cos 2\theta \rangle = 0$). Regarding the contractile strain generated in each contraction, CardioSlice constructs displayed higher strain rates compared with control constructs (Figure 3G), with a significantly higher ($p < 0.01$) average strain rate per beat (Figure 3H). Taken together, these results demonstrate that paced electrical stimulation of cardiac macrotissues over the 2 weeks of culture dramatically enhances contractile performance, and suggest improved maturation at the tissue level under these conditions.

CardioSlice Constructs Generate ECG-like Signals

Human cardiac macrotissues produced a bioelectrical signal that was a sum of the action potentials generated by the individual cardiomyocytes constituting the construct. Such signals could be registered on the surface of constructs using the electrodes embedded within the perfusion chamber (Figure 4A). In control constructs the recorded electrical signals were of low amplitude and long duration, which is consistent with the incomplete synchronization of contractions visualized across the macrotissue (Video S2). In contrast, CardioSlice constructs elicited bioelectrical signals composed of narrow and steep waveforms that include the QRS complexes and repolarizing T waves, remarkably similar to those of standard surface ECG for human ventricular myocardium (Figure 4A). Moreover, ECG-like signals recorded from CardioSlice constructs were of statistically significantly higher amplitude, shorter QRS duration, and shorter QT interval than those of control constructs (Figures 4B–4D). These results indicate that cardiomyocytes within CardioSlice constructs are electrically better coupled than within control constructs, attaining the fast conduction velocity and improved action potential propagation characteristic of a functional syncytium.

We next tested whether cardiomyocytes within macrotissue constructs retained the ability to respond to positive and negative inotropic factors. Similar to iPSC-derived cardiomyocytes cultured under standard 2D conditions and to control macrotissue constructs (data not shown), CardioSlice constructs increased or decreased beating rate upon treatment with isoproterenol or carbachol, respectively (Figures 4E and 4F).

Prediction of Drug-Induced Cardiotoxicity Using CardioSlice Constructs

To investigate the ability of human cardiac macrotissues to predict drug-induced cardiotoxicity, we incubated macrotissues at day 14 of culture with sotalol, a human ether-a-go-go (hERG) potassium channel blocker and adrenergic antagonist. Upon 10 min of treatment, control cardiac macrotissues showed no consistent alterations in the frequency or morphology of ECG-like signals (Figures 5A and S5A), making it difficult to determine any drug effect. In contrast, CardioSlice constructs displayed a progressive decrease in beating frequency, consistent with sotalol action as adrenergic antagonist (Figure S5B). More importantly, we could detect features typical of arrhythmia, such as ectopic QRS, prolongation of RR intervals, and regular blockades (Figure 5B). These features appeared progressively, were more frequent over time of incubation with sotalol, and coincided with abnormal prolongation of the QT interval, which experienced increases greater than 20%

Figure 4. Electrocardiogram-like Signals Generated by Human Cardiac Macrotissues during Spontaneous Beating

(A) Representative electrocardiogram (ECG)-like signals (voltage recorded as a function of time). Left panel shows non-stimulated (Control) and electrically stimulated (CardioSlice) human cardiac macrotissues during spontaneous beating. Right panel shows the QRS complex and T wave over the averaged ECG-like beats (signals for 10 min were considered).

(B–D) Box plots showing the QRS complex duration (B), the QT interval duration (C), and the amplitude of the QRS complex (D) from the signals generated by human cardiac macrotissues. Each experimental pair (Control and CardioSlice) has been normalized by the corresponding mean CardioSlice value. Box plot represents median, 25%, and 75%, and whiskers correspond to maximum and minimum values (***$p < 0.001$, $N \geq 4$, $n \geq 4$ per group; F test).

(E and F) Representative ECG-like signals recorded from CardioSlice constructs before (first minute, black lines) and after (10-min incubation, light-gray lines) treatments with isoproterenol (E) and carbachol (F). Time intervals between two consecutive R peaks (RR) of QRS complexes are indicated by arrows. Bar charts show the change of the beat rate (defined as 1/RR) induced by isoproterenol and carbachol treatments. Data plotted show relative changes with respect to the mean beat rate value before treatment (baseline) for each experiment (average ± SEM) (***$p < 0.001$, $N = 3$, $n = 3$ per group; Mann-Whitney U test). All ECG-like bioelectric signals were bandpass filtered (zero-phase fourth-order Butterworth filter with cutoff frequency of 0.2 and 40 Hz, respectively).

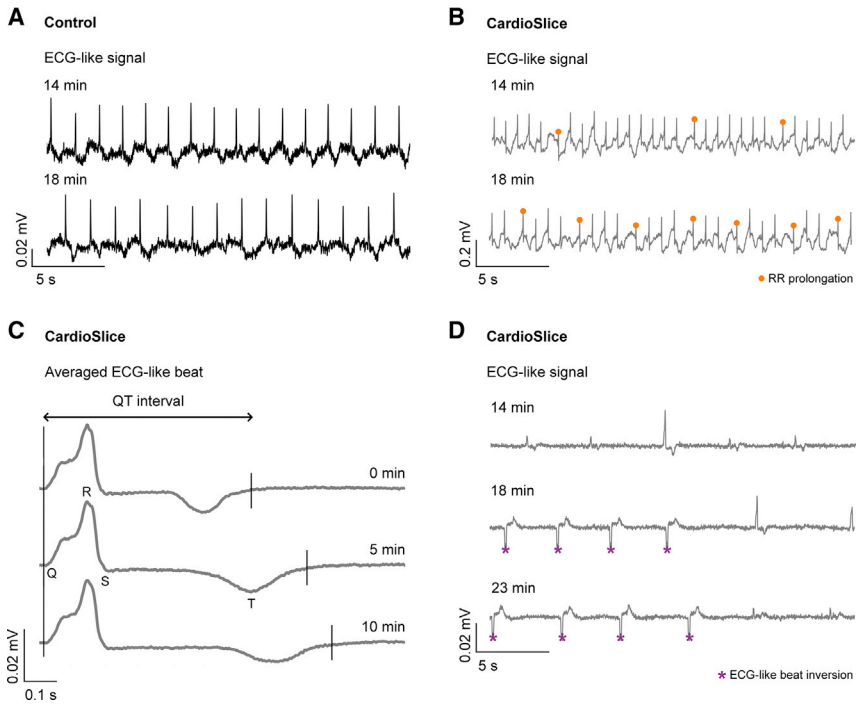

Figure 5. Effects of Sotalol on the ECG-like Signal of CardioSlice Constructs

(A, B, and D) Representative ECG-like signals for control (A) and CardioSlice (B and D) constructs cultured for 14 days after treatment with sotalol.

(A) ECG-like signals recorded from control constructs upon 14 and 18 min of treatment with sotalol.

(B) ECG-like signals recorded from CardioSlice constructs upon 14 and 18 min of treatment with sotalol. Prolongations in time intervals between two consecutive R peaks (RR) of QRS complex are represented by solid points.

(C) QT interval prolongation in CardioSlice constructs, estimated by signal averaging at basal conditions and after 5 and 10 min of incubation with sotalol. QT interval is shown over the averaged ECG-like signals at basal conditions by arrows. The QRS complex and T wave are also shown. The smaller vertical lines indicate the end of T wave. The effects of sotalol on the ECG-like of control and CardioSlice constructs were analyzed in four independent experiments (Control N = 4, n = 5; CardioSlice N = 4, n = 4).

(D) ECG-like signals for CardioSlice constructs upon 14, 18, and 23 min of treatment with sotalol. Inversion of ECG-like signals are represented by asterisks. All ECG-like bioelectric signals were bandpass filtered (zero-phase fourth-order Butterworth filter with cutoff frequency of 0.2 and 40 Hz, respectively).

(Figure 5C). After prolonged incubation times with sotalol, CardioSlice constructs displayed severe alterations in ECG-like signals, with QRS complexes becoming smaller, inverted, and even disappearing after 30 min of drug treatment (Figure 5D). The observed electrophysiological alterations translated, at the mechanical level, into dyssynchronous contractile patterns in sotalol-treated CardioSlice constructs (Figure S5B). Therefore, sotalol impaired the electrical conduction within CardioSlice constructs and affected their contractile behavior, demonstrating the proarrhythmic potential of the drug. On the whole, these results indicate that CardioSlice constructs are suitable *in vitro* models for prediction of drug-induced cardiotoxicity.

DISCUSSION

Environmental cues are key determinants of cardiomyocyte phenotype and function, and regulate their capacity to form functional tissue units. Despite recent advances, *in vitro* generation of human heart tissue is still limited by the existing tissue-engineering technologies, which are not able to recapitulate the complex structure and function of the human myocardium. Electrical stimulation, alone or in combination with mechanical loading, has been widely applied in tissue engineering to generate cardiac constructs that recapitulate some aspects of the native physiology (Godier-Furnemont et al., 2015; Nunes et al., 2013). Electrical pacing has also been applied to the generation of human cardiac microtissues (Nunes et al., 2013; Ruan et al., 2016; Thavandiran et al., 2013; Xiao et al., 2014). Such microtissues are usually fabricated by using cell-laden natural-based hydrogels cast on posts (Fennema et al., 2013; Hinson et al., 2015; Huebsch et al., 2016; Kensah et al., 2013; Ruan et al., 2016; Schaaf et al., 2011; Soong et al., 2012; Thavandiran et al., 2013; Tiburcy et al., 2017; Turnbull et al., 2014; Zhang et al., 2013) or around a wire template (Nunes et al., 2013; Xiao et al., 2014). While some of those constructs could be quite large in surface area, even larger than ours (Nakane et al., 2017; Shadrin et al., 2017; Tiburcy et al., 2017), their thickness was constrained by the ~300-μm limit of oxygen diffusion in passive culture systems (Lovett et al., 2009). To overcome such size limitation, the production of thicker cardiac constructs can be then performed by medium perfusion bioreactors, which are able to maintain cell viability over time (Radisic et al., 2008). Perfusion bioreactors incorporating electrical

stimulation have been previously applied for *in vitro* culture of murine cardiomyocyte 3D tissue structures (Barash et al., 2010; Kensah et al., 2011; Maidhof et al., 2012). However, this research had been rarely transferred to human cardiac tissue-engineering models (Ma et al., 2014; Tiburcy et al., 2017) and not previously used to combine iPSC-derived cells and 3D thick scaffolds with simultaneous perfusion and electrical stimulation to develop macrotissues of human cardiomyocytes. Herein, we have developed a parallelized bioreactor system equipped with electrodes to electrically stimulate human iPSC-derived cardiomyocytes during perfusion in culture.

Electrical stimulation has been proposed to be a requirement for the electrophysiological maturation of cardiac constructs, favoring cardiomyocyte contractility, alignment, and organization within cardiac tissue constructs (Nunes et al., 2013; Radisic et al., 2004a). In our case, after 14 days in culture, cardiomyocytes in CardioSlice constructs displayed small, but measurable, signs of increased cell maturation compared with control constructs, showing wider sarcomeres and more developed intercellular unions (Figures 2C and 2D). Nevertheless, the expression levels of maturity-related cardiac genes and cardiac ion channels indicated immature fetal-like cardiomyocyte characteristics, still far from those of adult myocardium (Figure S3D). Notably, however, continuous electrical stimulation did have a profound effect on the properties of CardioSlice constructs at the tissue level, resulting in greatly improved electromechanical coupling. We believe that the implications of these findings are important in two respects: First, our findings illustrate a viable approach to engineering human myocardial surrogates with value for cardiac toxicity testing. In this respect, most previous studies aimed at producing adult-like cardiac constructs focused on increasing the degree of maturation of cardiomyocytes (with only relative success to date: see Nunes et al., 2013; Ronaldson-Bouchard et al., 2018; Ruan et al., 2016; Tiburcy et al., 2017), while our findings highlight the usefulness of promoting the maturation at the tissue level, in a way that supersedes and does not strictly depend on the maturation at the cellular level. Second, on a more conceptual note, our findings provide experimental support for the appearance of emergent behaviors in the context of a complex system (Gao et al., 2018) such as myocardial tissue organization and function, where relatively small changes in the properties of the system elements (cardiomyocytes) can lead to higher-order behaviors at greater scales (tissue). In the case of myocardial tissue this appears to be particularly relevant, probably because of the system's normal operation as a functional syncytium (Hunter et al., 2003). Tissue-like maturation of CardioSlice constructs resulted in contractions with an amplitude 6-fold higher than that of control constructs. Moreover, ECG-like signals elicited by CardioSlice constructs showed a uniform and reproducible pattern of narrow, steep, and well-defined QRS complexes that very much resembled actual ECG heart recordings. In contrast with CardioSlice constructs, the bioelectrical signals generated by control constructs were highly heterogeneous, of comparatively lower amplitude and longer duration of waveforms, indicative of slowly conducting tissues.

By incorporating electrodes in our bioreactor chamber, we were able to not only stimulate our constructs but also provide the system with the capability of on-line monitoring of the electrophysiological behavior of thick cardiac constructs in a non-destructive manner. As no standard method exists for the assessment of electrophysiological information from intact macroscale-sized heart tissue (Tzatzalos et al., 2016), the technology developed here is unique in this context. The bioelectrical signal obtained in this way is extremely informative of the electrically active cells within the construct and, most importantly, of the intercellular coupling at the macro (whole construct) scale, very similar to the case of surface ECG recordings in humans.

Typically, safety of cardiac drugs is assessed by measuring currents on hERG ion channels ectopically expressed in non-cardiac cell lines (HEK293, CHO). These assays produce false positives and false negatives, as in the cases of verapamil and alfuzosin, respectively (Mathur et al., 2015). Our system allowed us to determine the effects of proarrhythmic drugs on the ECG-like signal generated by CardioSlice constructs. Upon treatment with the proarrhythmic drug sotalol, CardioSlice constructs showed a pathological prolongation of the QT interval, and alterations in the morphology and polarity of the QRS complex in ECG-like signals and arrhythmias, as seen *in vivo* (Straus et al., 2006). Such responses were not identified in control constructs, even though they contained the same numbers of cardiomyocytes and fibroblasts, cultured in parallel under identical conditions (except, of course, for the continuous electrical stimulation applied to CardioSlice constructs). Because the proarrhythmic behavior of drugs is often only found after they have been administered to patients, we propose that the predictive capabilities of CardioSlice constructs reflect their higher degree of close-to-human tissue-like functionality.

In summary, the novelty of our studies is twofold. On the one hand, we have developed a method and associated technology for the production of thick human cardiac macrotissues, with capabilities for electric stimulation and on-line electrophysiological recording. On the other hand, our findings show that continuous electrical stimulation of cardiac macrotissues resulted in minor (albeit measurable) improvements in cardiomyocyte maturation, but greatly enhanced maturation at the tissue level.

CardioSlice constructs showed superior electromechanical coupling and were able to predict drug-induced cardiotoxicity, illustrating the enhanced tissue-like functionality achieved by our model. The physiological relevance of CardioSlice constructs, together with their parallel and scalable nature and the on-line electrophysiological monitoring feature, take our technology to the forefront of the production of engineered human cardiac macrotissues.

EXPERIMENTAL PROCEDURES

Experimental procedures are provided in detail in Supplemental Information.

Use of Human and Animal Subjects

The use of animals for experimentation in these studies was done following a protocol approved by the Animal Experimentation Ethics Committee of the University of Barcelona (Barcelona, Spain). The use of human iPSCs in this work was approved by the Spanish competent authorities (Commission on Guarantees concerning the Donation and Use of Human Tissues and Cells of the Carlos III Spanish National Institute of Health).

Design, Fabrication, and Characterization of the Perfusion Chamber and Bioreactor System

Custom-made perfusion chambers with electrical stimulation and parallel bioreactors for continuous perfusion were designed and fabricated as described in Supplemental Information.

Generation of Engineered Human Cardiac Macrotissues

Cardiomyocytes were differentiated from hiPSCs (FiPS Ctrl1-mR5F-6; cell line registered in the National Stem Cell Bank, Carlos III Spanish National Institute of Health) as described in Supplemental Information, and seeded into porous collagen- and elastin-based scaffolds of 1-mm thickness in dry conditions (Matriderm). Detailed methods are provided in Supplemental Information.

Morphological, Functional, and Molecular Analyses

Immunostaining, flow cytometry, qRT-PCR, confocal and electron microscopy, contractility analyses, and electrophysiological recording and processing of cardiac macrotissues were performed as described in Supplemental Information.

Statistical Analyses

The number of replicated measurements per experiment (n) and of independent experiments (N) is specified in the figure legends. Normal distribution of data was tested using the Shapiro-Wilk and Kolmogorov-Smirnov normality tests. In the case of normal distributions, comparisons between experiments involving two groups were performed using Student's t test (Figures S1A, S3B, and S3C). Non-parametric analyses were performed using the Mann-Whitney *U* test for sarcomere width (Figure 2D), fractional area change (Figure 3C), MCR (Figure 3D), and $\langle \cos 2\theta \rangle$ (Figure 3F), as well as to evaluate the beating-rate change after drug treatments (Figures 4E and 4F). Regarding the average strain per contraction (Figure 3H) and for experiments involving more than two groups (gene expression analysis), data were analyzed using one-way ANOVA followed by a post hoc Tukey's test. The difference between the variance of experimental groups in QRS duration, QT interval, and QRS amplitude (Figures 4B–4D) was analyzed using two-sample test for variances (F test), and data were normalized to electrical pacing conditioning. Software used were Origin 8.5 (OriginLab, Northampton, USA) and GraphPad Prism 6, and differences were considered significant when $p < 0.05$.

SUPPLEMENTAL INFORMATION

Supplemental Information can be found online at https://doi.org/10.1016/j.stemcr.2019.05.024.

AUTHOR CONTRIBUTIONS

E.M. and A.R. conceived the study and supervised the project. M.V.-M., O.I.-G., R.J., E.M., and A.R. planned experiments. M.V.-M., O.I.-G., C.D.G., L.S., K.T., R.P., J.C., D.B.-A., S.J.-D., O.C.-F., and R.J. performed experiments. J.S. provided research advice. M.V.-M., O.I.-G., E.M., and A.R wrote the manuscript with contributions from all the authors.

ACKNOWLEDGMENTS

The authors would like to thank L. Mulero, C. Pardo, and C. Casal for excellent technical assistance with histological analysis and J.M. Vaquero for assistance with flow-cytometry analysis. We thank J. Martín from Leventon S.A.U. (WerfenLife Company) for kindly donating parts from the elastomeric infusion system DOSI-FUSER. This work was supported by grants from the Spanish Ministry of Economy and Competitiveness-MINECO (RTI2018-095377-B-100 and Severo Ochoa Program for Centers of Excellence in R&D 2016-2019) and Departament de Salut, Generalitat de Catalunya (PERIS SLT002/16/00234). Additional support was provided by grants from Instituto de Salud Carlos III-ISCIII/FEDER (Red de Terapia Celular - TerCel RD16/0011/0024), ACCIÓ/FEDER (AdvanceCat), Generalitat de Catalunya-AGAUR (2017-SGR-1079, 2017-SGR-1770, and 2017-SGR-899), Fundació la Marató de TV3 (201534-30), and CERCA Programme/Generalitat de Catalunya.

Received: May 17, 2018
Revised: May 23, 2019
Accepted: May 24, 2019
Published: June 20, 2019

REFERENCES

Amano, Y., Nishiguchi, A., Matsusaki, M., Iseoka, H., Miyagawa, S., Sawa, Y., Seo, M., Yamaguchi, T., and Akashi, M. (2016). Development of vascularized iPSC derived 3D-cardiomyocyte tissues by filtration layer-by-layer technique and their application for pharmaceutical assays. Acta Biomater. *33*, 110–121.

Bacabac, R.G., Smit, T.H., Cowin, S.C., Van Loon, J.J., Nieuwstadt, F.T., Heethaar, R., and Klein-Nulend, J. (2005). Dynamic shear stress in parallel-plate flow chambers. J. Biomech. *38*, 159–167.

Barash, Y., Dvir, T., Tandeitnik, P., Ruvinov, E., Guterman, H., and Cohen, S. (2010). Electric field stimulation integrated into perfusion bioreactor for cardiac tissue engineering. Tissue Eng. Part C Methods *16*, 1417–1426.

Carrier, R.L., Rupnick, M., Langer, R., Schoen, F.J., Freed, L.E., and Vunjak-Novakovic, G. (2002). Perfusion improves tissue architecture of engineered cardiac muscle. Tissue Eng. *8*, 175–188.

Cheng, M., Moretti, M., Engelmayr, G.C., and Freed, L.E. (2009). Insulin-like growth factor-I and slow, bi-directional perfusion enhance the formation of tissue-engineered cardiac grafts. Tissue Eng. Part A *15*, 645–653.

Chien, K.R., Domian, I.J., and Parker, K.K. (2008). Cardiogenesis and the complex biology of regenerative cardiovascular medicine. Science *322*, 1494–1497.

Fennema, E., Rivron, N., Rouwkema, J., van Blitterswijk, C., and de Boer, J. (2013). Spheroid culture as a tool for creating 3D complex tissues. Trends Biotechnol. *31*, 108–115.

Feric, N.T., and Radisic, M. (2016). Maturing human pluripotent stem cell-derived cardiomyocytes in human engineered cardiac tissues. Adv. Drug Deliv. Rev. *96*, 110–134.

Fermini, B., and Fossa, A.A. (2003). The impact of drug-induced QT interval prolongation on drug discovery and development. Nat. Rev. Drug Discov. *2*, 439–447.

Fleischer, S., Shapira, A., Feiner, R., and Dvir, T. (2017). Modular assembly of thick multifunctional cardiac patches. Proc. Natl. Acad. Sci. U S A *114*, 1898–1903.

Gao, L., Gregorich, Z.R., Zhu, W., Mattapally, S., Oduk, Y., Lou, X., Kannappan, R., Borovjagin, A.V., Walcott, G.P., Pollard, A.E., et al. (2018). Large cardiac muscle patches engineered from human induced-pluripotent stem cell-derived cardiac cells improve recovery from myocardial infarction in swine. Circulation *137*, 1712–1730.

Godier-Furnemont, A.F., Tiburcy, M., Wagner, E., Dewenter, M., Lammle, S., El-Armouche, A., Lehnart, S.E., Vunjak-Novakovic, G., and Zimmermann, W.H. (2015). Physiologic force-frequency response in engineered heart muscle by electromechanical stimulation. Biomaterials *60*, 82–91.

Hansen, A., Eder, A., Bonstrup, M., Flato, M., Mewe, M., Schaaf, S., Aksehirlioglu, B., Schwoerer, A.P., Uebeler, J., and Eschenhagen, T. (2010). Development of a drug screening platform based on engineered heart tissue. Circ. Res. *107*, 35–44.

Hinson, J.T., Chopra, A., Nafissi, N., Polacheck, W.J., Benson, C.C., Swist, S., Gorham, J., Yang, L., Schafer, S., Sheng, C.C., et al. (2015). HEART DISEASE. Titin mutations in iPS cells define sarcomere insufficiency as a cause of dilated cardiomyopathy. Science *349*, 982–986.

Huebsch, N., Loskill, P., Deveshwar, N., Spencer, C.I., Judge, L.M., Mandegar, M.A., Fox, C.B., Mohamed, T.M., Ma, Z., Mathur, A., et al. (2016). Miniaturized iPS-cell-derived cardiac muscles for physiologically relevant drug response analyses. Sci. Rep. *6*, 24726.

Hunter, P.J., Pullan, A.J., and Smaill, B.H. (2003). Modeling total heart function. Annu. Rev. Biomed. Eng. *5*, 147–177.

Kensah, G., Gruh, I., Viering, J., Schumann, H., Dahlmann, J., Meyer, H., Skvorc, D., Bar, A., Akhyari, P., Heisterkamp, A., et al. (2011). A novel miniaturized multimodal bioreactor for continuous in situ assessment of bioartificial cardiac tissue during stimulation and maturation. Tissue Eng. Part C Methods *17*, 463–473.

Kensah, G., Roa Lara, A., Dahlmann, J., Zweigerdt, R., Schwanke, K., Hegermann, J., Skvorc, D., Gawol, A., Azizian, A., Wagner, S., et al. (2013). Murine and human pluripotent stem cell-derived cardiac bodies form contractile myocardial tissue in vitro. Eur. Heart J. *34*, 1134–1146.

Kurokawa, Y.K., and George, S.C. (2016). Tissue engineering the cardiac microenvironment: multicellular microphysiological systems for drug screening. Adv. Drug Deliv. Rev. *96*, 225–233.

Lian, X., Zhang, J., Azarin, S.M., Zhu, K., Hazeltine, L.B., Bao, X., Hsiao, C., Kamp, T.J., and Palecek, S.P. (2013). Directed cardiomyocyte differentiation from human pluripotent stem cells by modulating Wnt/beta-catenin signaling under fully defined conditions. Nat. Protoc. *8*, 162–175.

Liau, B., Jackman, C.P., Li, Y., and Bursac, N. (2017). Developmental stage-dependent effects of cardiac fibroblasts on function of stem cell-derived engineered cardiac tissues. Sci. Rep. *7*, 42290.

Lovett, M., Lee, K., Edwards, A., and Kaplan, D.L. (2009). Vascularization strategies for tissue engineering. Tissue Eng. Part B Rev. *15*, 353–370.

Ma, Z., Koo, S., Finnegan, M.A., Loskill, P., Huebsch, N., Marks, N.C., Conklin, B.R., Grigoropoulos, C.P., and Healy, K.E. (2014). Three-dimensional filamentous human diseased cardiac tissue model. Biomaterials *35*, 1367–1377.

Ma, Z., Wang, J., Loskill, P., Huebsch, N., Koo, S., Svedlund, F.L., Marks, N.C., Hua, E.W., Grigoropoulos, C.P., Conklin, B.R., et al. (2015). Self-organizing human cardiac microchambers mediated by geometric confinement. Nat. Commun. *6*, 7413.

Maidhof, R., Tandon, N., Lee, E.J., Luo, J., Duan, Y., Yeager, K., Konofagou, E., and Vunjak-Novakovic, G. (2012). Biomimetic perfusion and electrical stimulation applied in concert improved the assembly of engineered cardiac tissue. J. Tissue Eng. Regen. Med. *6*, e12–23.

Mathur, A., Loskill, P., Shao, K., Huebsch, N., Hong, S., Marcus, S.G., Marks, N., Mandegar, M., Conklin, B.R., Lee, L.P., et al. (2015). Human iPSC-based cardiac microphysiological system for drug screening applications. Sci. Rep. *5*, 8883.

Nakane, T., Masumoto, H., Tinney, J.P., Yuan, F., Kowalski, W.J., Ye, F., LeBlanc, A.J., Sakata, R., Yamashita, J.K., and Keller, B.B. (2017). Impact of cell composition and geometry on human induced pluripotent stem cells-derived engineered cardiac tissue. Sci. Rep. *7*, 45641.

Nunes, S.S., Miklas, J.W., Liu, J., Aschar-Sobbi, R., Xiao, Y., Zhang, B., Jiang, J., Masse, S., Gagliardi, M., Hsieh, A., et al. (2013). Biowire: a platform for maturation of human pluripotent stem cell-derived cardiomyocytes. Nat. Methods *10*, 781–787.

Parsa, H., Ronaldson, K., and Vunjak-Novakovic, G. (2016). Bioengineering methods for myocardial regeneration. Adv. Drug Deliv. Rev. *96*, 195–202.

Radisic, M., Marsano, A., Maidhof, R., Wang, Y., and Vunjak-Novakovic, G. (2008). Cardiac tissue engineering using perfusion bioreactor systems. Nat. Protoc. *3*, 719–738.

Radisic, M., Park, H., Shing, H., Consi, T., Schoen, F.J., Langer, R., Freed, L.E., and Vunjak-Novakovic, G. (2004a). Functional assembly

of engineered myocardium by electrical stimulation of cardiac myocytes cultured on scaffolds. Proc. Natl. Acad. Sci. U S A *101*, 18129–18134.

Radisic, M., Yang, L., Boublik, J., Cohen, R.J., Langer, R., Freed, L.E., and Vunjak-Novakovic, G. (2004b). Medium perfusion enables engineering of compact and contractile cardiac tissue. Am. J. Physiol. Heart Circ. Physiol. *286*, H507–H516.

Ronaldson-Bouchard, K., Ma, S.P., Yeager, K., Chen, T., Song, L., Sirabella, D., Morikawa, K., Teles, D., Yazawa, M., and Vunjak-Novakovic, G. (2018). Advanced maturation of human cardiac tissue grown from pluripotent stem cells. Nature *556*, 239–243.

Ruan, J.L., Tulloch, N.L., Razumova, M.V., Saiget, M., Muskheli, V., Pabon, L., Reinecke, H., Regnier, M., and Murry, C.E. (2016). Mechanical stress conditioning and electrical stimulation promote contractility and force maturation of induced pluripotent stem cell-derived human cardiac tissue. Circulation *134*, 1557–1567.

Schaaf, S., Shibamiya, A., Mewe, M., Eder, A., Stohr, A., Hirt, M.N., Rau, T., Zimmermann, W.H., Conradi, L., Eschenhagen, T., et al. (2011). Human engineered heart tissue as a versatile tool in basic research and preclinical toxicology. PLoS One *6*, e26397.

Shachar, M., Benishti, N., and Cohen, S. (2012). Effects of mechanical stimulation induced by compression and medium perfusion on cardiac tissue engineering. Biotechnol. Prog. *28*, 1551–1559.

Shadrin, I.Y., Allen, B.W., Qian, Y., Jackman, C.P., Carlson, A.L., Juhas, M.E., and Bursac, N. (2017). Cardiopatch platform enables maturation and scale-up of human pluripotent stem cell-derived engineered heart tissues. Nat. Commun. *8*, 1825.

Shimizu, T., Yamato, M., Isoi, Y., Akutsu, T., Setomaru, T., Abe, K., Kikuchi, A., Umezu, M., and Okano, T. (2002). Fabrication of pulsatile cardiac tissue grafts using a novel 3-dimensional cell sheet manipulation technique and temperature-responsive cell culture surfaces. Circ. Res. *90*, e40.

Soong, P.L., Tiburcy, M., and Zimmermann, W.H. (2012). Cardiac differentiation of human embryonic stem cells and their assembly into engineered heart muscle. Curr. Protoc. Cell Biol. Chapter 23, Unit 23.8. https://doi.org/10.1002/0471143030.cb2308s55.

Straus, S.M., Kors, J.A., De Bruin, M.L., van der Hooft, C.S., Hofman, A., Heeringa, J., Deckers, J.W., Kingma, J.H., Sturkenboom, M.C., Stricker, B.H., et al. (2006). Prolonged QTc interval and risk of sudden cardiac death in a population of older adults. J. Am. Coll. Cardiol. *47*, 362–367.

Tandon, N., Cannizzaro, C., Chao, P.H., Maidhof, R., Marsano, A., Au, H.T., Radisic, M., and Vunjak-Novakovic, G. (2009). Electrical stimulation systems for cardiac tissue engineering. Nat. Protoc. *4*, 155–173.

Thavandiran, N., Dubois, N., Mikryukov, A., Masse, S., Beca, B., Simmons, C.A., Deshpande, V.S., McGarry, J.P., Chen, C.S., Nanthakumar, K., et al. (2013). Design and formulation of functional pluripotent stem cell-derived cardiac microtissues. Proc. Natl. Acad. Sci. U S A *110*, E4698–E4707.

Tiburcy, M., Hudson, J.E., Balfanz, P., Schlick, S., Meyer, T., Chang Liao, M.L., Levent, E., Raad, F., Zeidler, S., Wingender, E., et al. (2017). Defined engineered human myocardium with advanced maturation for applications in heart failure modeling and repair. Circulation *135*, 1832–1847.

Turnbull, I.C., Karakikes, I., Serrao, G.W., Backeris, P., Lee, J.J., Xie, C., Senyei, G., Gordon, R.E., Li, R.A., Akar, F.G., et al. (2014). Advancing functional engineered cardiac tissues toward a preclinical model of human myocardium. FASEB J. *28*, 644–654.

Tzatzalos, E., Abilez, O.J., Shukla, P., and Wu, J.C. (2016). Engineered heart tissues and induced pluripotent stem cells: macro- and microstructures for disease modeling, drug screening, and translational studies. Adv. Drug Deliv. Rev. *96*, 234–244.

Xiao, Y., Zhang, B., Liu, H., Miklas, J.W., Gagliardi, M., Pahnke, A., Thavandiran, N., Sun, Y., Simmons, C., Keller, G., et al. (2014). Microfabricated perfusable cardiac biowire: a platform that mimics native cardiac bundle. Lab Chip *14*, 869–882.

Yang, X., Pabon, L., and Murry, C.E. (2014). Engineering adolescence: maturation of human pluripotent stem cell-derived cardiomyocytes. Circ. Res. *114*, 511–523.

Zhang, D., Shadrin, I.Y., Lam, J., Xian, H.Q., Snodgrass, H.R., and Bursac, N. (2013). Tissue-engineered cardiac patch for advanced functional maturation of human ESC-derived cardiomyocytes. Biomaterials *34*, 5813–5820.

Zimmermann, W.H., Schneiderbanger, K., Schubert, P., Didie, M., Munzel, F., Heubach, J.F., Kostin, S., Neuhuber, W.L., and Eschenhagen, T. (2002). Tissue engineering of a differentiated cardiac muscle construct. Circ. Res. *90*, 223–230.